

Role of Hydrophobic Patch in LRP6: A Promising Drug Target for Alzheimer's disease

K. MUTHUSAMY*, S. PRASAD AND S. NAGAMANI

Department of Bioinformatics, Science Block, Alagappa University, Karaikudi-630 004, India

Muthusamy, *et al.*: Hydrophobic Patch in LRP6 for Alzheimer's disease

Alzheimer's disease is one of the most fatal dementia occurring in elderly persons. LRP6 and DKK1 proteins are found in the senile plaques of Alzheimer's disease patients. Inducing the disassociation/inhibition of the LRP6–DKK1 complex is a vital mechanism for the treatment of Alzheimer's disease. This study accomplished its goal of targeting potent inhibitors against LRP6 by molecular modeling techniques such as high throughput virtual screening and molecular dynamics simulations. Zinc database compounds were docked in the hydrophobic patch of LRP6 and in the active site of DKK1 using the GLIDE module. The initial docking results were well exemplified to amino acid residues interacting on the hydrophobic patch of LRP6 and active sites of DKK1. Further, the best hit compounds (866) were again redocked with Glide XP and finally six lead compounds were identified as the best inhibitors against LRP6 which was later confirmed by molecular dynamics simulation studies.

Key words: Alzheimer's disease, late onset AD, LRP6, DKK1, HTVS, Molecular Dynamics simulations

Alzheimer's disease (AD) is an accelerating neurodegenerative disorder characterized by an intense shortfall of cognitive processes that divulge as alterations in the memory, judgment, and reasoning^[1]. Microgliosis, dystrophic neuritis and loss of neurons and synapses are the main pathological manifestations of AD^[2]. The worldwide prevalence of AD is estimated to be 24 million with 5.5 million people in the US^[3]. Nearly 4.6 million new cases of AD are reported every year^[4]. Between the ages of 60 and 85 years, there is almost a 15-fold increase in the prevalence of dementia, especially in AD^[5]. The prevalence of AD is higher in the US compared to Africa, Asia, and Europe. African-Americans and Hispanics are known to be affected more with AD than the native Africans in their homelands^[6].

Genetic and biochemical studies of AD reveal its association with low density lipoprotein receptor related protein (LRP). Late onset AD (LOAD) is associated with a single base pair change within exon 3 (C766T) and polymorphisms in the LRP gene on chromosome 12 in a 5' tetra nucleotide repeat^[7]. Meanwhile in senile plaques, there have been reports of LRP and its ligands^[8]. Amyloid precursor protein (APP) is interacted with LRP in neurons influences the APP processing and metabolism, and thereby the production of A β , an important aspect in the pathogenesis of AD^[9]. The A β are regulated by LRP ligands, α 2M and apoE^[10].

The role of the single polypeptide precursor is

very important in the synthesis of LRP6, which is processed into two heterodimeric peptides by furinin trans-Golgi network^[11]. There is a non-covalent association of 85 kDa transmembrane and cytoplasmic light-chain coupled to heavy-chain of LRP6 (515 kDa). The light-chain contains four ligand-binding domains (clusters I-IV) consisting of 2, 8, 10, and 11 cysteine-rich complement type repeats, respectively. Clusters I-IV (ligand-binding domains), epidermal growth factor (EGF) receptor-like repeats, and YWTD-propeller repeats are a part of light-chain of LRP6^[12].

Earlier, there was no reported inhibitor against the hydrophobic patch of LRP6 for AD. LRP6 potent inhibitors are able to work against LOAD. It is confirmed from crystallographic studies that the hydrophobic patches on the top surfaces of LRP6 E1 and E3 are the core part of LRP6-DKK1 interaction sites. Thus, hydrophobic patches on the LRP6 which target the Wnt/ β -catenin pathway, are able to become strong inhibitors against LOAD^[13].

Previously our group has identified few plant compounds against APOE4 to treat AD^[14]. In this study, an initial attempt was made to formulate a protocol for a structure-based drug-design approach that targets LRP6 in the canonical β -catenin pathway. Zinc database compounds (~727,842 compounds) were docked in the active site of the LRP6-DKK1 interaction core. Sequential docking method (HTVS, SP and XP) and subsequent molecular dynamics simulation were performed. The results from this study pave the way to design potent inhibitors to treat LOAD.

*Address for correspondence

E-mail: mkbioinformatics@gmail.com

MATERIALS AND METHODS

All computation analyses were carried out on Centos 6.2 Linux platform in Intel core 2 duo processor with a 4 GB RAM.

Protein preparation:

The complex structure of LRP6 and DKK1 conjugated form (PDB ID–3S8V) was retrieved from the RCSB Protein Data Bank^[15] and imported to the protein preparation wizard. Initially, polar hydrogen atoms were added and unwanted water molecules were removed from the structure. The structure was further optimized and energy was minimized by restrained minimization by assigning RMSD 0.30Å. Partial charges were added with the help of optimized potentials liquid for simulations_2005 (OPLS_2005) force field^[16].

Ligand structure preparation:

In the next step, the zinc database compounds were prepared for docking analysis. Initially all the two-dimensional (2D) SDF format was converted into 3D Maestro format by the LigPrep module. In the subsequent steps, various tautomers and ring conformations were generated and an approximate conformational energy was calculated by the OPLS_2005 force field^[17].

Receptor grid generation:

Hydrophobic patches on the top surface of LRP6-E1E3 are formed by the residues Ile681, Tyr706, Trp767, Phe836, Trp850, Tyr875 and Met877. A grid was made around the LRP6-DKK1 core interaction site by the above mentioned residues. This hydrophobic interaction is buttressed by several salt bridges and hydrogen bonds between LRP6-E3 and DKK1c:LRP6 Glu708 with DKK1 His204, LRP6 Arg792 with DKK1 Glu232, LRP6 Asp811 with DKK1 Arg236, and LRP6 His834 with DKK1 Ser228^[13]. The atoms were scaled by van der Waals radii of 1.0 Å with the partial atomic charge less than 0.25 defaults.

High throughput virtual screening and docking:

Zinc database (nearly 727842 compounds) compounds were docked in the active site of LRP6 and DKK1 to find cogent inhibitors against the hydrophobic patch on the LRP6. Suitable protonations were assigned to all the ligands with the help of the LigPrep program at physiological pH of 7.2 ± 0.2 . Docking analysis was done in the GLIDE module^[18] which is explicitly defined to search for possible locations in the active-site region of the protein. First, all the zinc database

compounds were docked in the active sites of LRP6 and DKK1 separately by HTVS (High Throughput Virtual Screening). Nearly 1000 compounds had good Glide scores. Further, these compounds were screened by SP (Standard Precision) followed by XP (Extra Precision) mode of docking. On the basis of the best Glide scores and Glide energies, six best compounds were identified as potential lead molecules. The docking parameters were already discussed in detail in our previous publications^[19,20].

ADME screening:

Absorption distribution metabolism excretion/toxicity (ADME/T) properties of the screened compounds were inferred by the QikProp program^[21] which not only identifies the physically significant descriptors but also the pharmaceutically relevant properties. Before being submitted to the QikProp program, all compounds were neutralized. Overall, it analysed 44 properties for the molecules with a wide area of physiochemical properties including log P (octanol/water), QP%, and log HERG. Evaluation of the acceptability of compounds was confirmed on the basis of different physiochemical properties such as Lipinski's rule of 5^[22], which is indispensable for a rational drug design.

Molecular dynamics simulation:

Molecular dynamics simulations were performed for the six different protein-ligand complexes (LRP6_71404536, LRP6_3116518, LRP6_67911943, LRP6_04349511, LRP6_70665802 and LRP6_67903416) and (DKK1_71404536, DKK1_3116518, DKK1_67911943, DKK1_04349511, DKK1_70665802 and DKK1_67903416). All molecular dynamics simulation studies were performed in the GROMACS 4.5.5 software^[23]. Gromos 43a1 force field, NVT and NPT ensemble were applied to the system. The model was solvated by simple point charge water molecules (SPC/E) and it was placed at the center of a $72 \text{ \AA} \times 72 \text{ \AA} \times 72 \text{ \AA}$ cubic box. The simulated system was made electrically neutral by replacing the water molecules with six Na^+ counter ions. Long-range electrostatic interactions were accurately determined by the particle mesh Ewald (PME) method^[24]. Fast Fourier transform calculation with a grid spacing of 1.2 Å and vdW interactions with a cut-off of 9 Å were applied. A constant temperature and pressure for the whole system (300 K and 1 bar) was achieved with the Berendsen thermostat^[25] and the Parrinello and Rahman^[26] barostat parameters. Steepest descent energy minimization process^[27] was utilized to minimize the simulated system step-by-step until a

tolerance of 1000 kJ/mol was achieved. A pH of 7 was maintained for all the molecular dynamics simulation processes. Bond constraints were provided by the LINC algorithm^[28]. Five nanoseconds molecular dynamics simulations were performed and the coordinates were generated for every 2 fs.

RESULTS AND DISCUSSION

LRP6 is an important receptor in the *Wnt*/β catenin canonical pathway where DKK1 binds in the normal state as a natural antagonist. While in the extreme level of disease, DKK1 unbinds from the LRP6, giving privilege for *Wnt* signaling pathway to activate the TCF/LEF genes. In order to check the effectiveness of the ligands, docking was performed on the active site of DKK1 and on the hydrophobic patch of LRP6 where DKK1 binds. Ligands interacting on the active site of DKK1 and residues interacting on the hydrophobic patch of LRP6 were confirmed based on good Glide score and Glide energy. Ligands can bind to the active site of the hydrophobic patch on LRP6 with the same efficacy as DKK1 binds to LRP6 as a natural antagonist.

In the subsequent steps, molecular dynamics simulations were also performed on the LRP6 and DKK1 ligand complexes separately. RMSD, radius of gyration, number of hydrogen bonds and SASA were analyzed to determine the structure and ligand flexibility. Molecular dynamics studies proved the potency of ligands as the best inhibitors against LOAD.

HTVS was performed against a zinc database which contained 727 842 compounds^[29]. A number of rotatable bonds, LogP values were annotated and biologically relevant protonation states were assigned to the molecules. In this library, all the compounds were assigned to multiple protonation states and multiple conformation and tautomeric forms.

Molecular docking has two important functions; first, sampling of conformations of small compounds at protein-binding sites and second, assessing the protein binding sites by scoring functions. Three different docking steps used to find the best inhibitors are HTVS, SP, and XP mode. In the beginning, all the dataset compounds were docked at the LRP6-DKK1 active site by the Glide HTVS method as it consumes less CPU time. We screened all the 727 842 compounds through this process. Further, these compounds went through stepwise SP and XP mode of docking. Finally, 866 compounds were screened by the Glide XP mode of docking. On the basis of docking scores and glide energy scores, six

best compounds were identified as potential lead molecules against LRP6.

The binding site for the two molecular targets, including LRP6 and DKK1 (PDB ID - 3S8V) were identified by the literature. The predicted amino acids were Arg639, Ile681, Tyr706, Trp767, Phe836, Trp850, Tyr875, and Met877 on the hydrophobic patch of LRP6 and ligands. While the amino acids interacted with the DKK1 and ligands were identified to be His204, Phe205, Trp206, Leu231, Glu232, Ile233, Phe234, and Arg236. Chemical name of all the six lead compounds and their corresponding database id numbers are: ZINC71404536 - (2E)-2-[(3,4-dihydroxyphenyl)methylene]-7-hydroxy-6-[(2S,3R,4R,5S,6S)-3,4,5-trihydroxy-6-(hydroxymethyl)], ZINC04349511 - 2-{4-[(2S,5S)-3,4,5-trihydroxy-6-(hydroxymethyl)(2H-3,4,5,6-tetrahydropyran-2-yloxy)]-3-hydroxyphenyl}-5,7-dihydroxy chromen-4-one, ZINC31165518 - (2S,3R,4S,5R)-2-[[[(3S)-1,7-bis(3,4-dihydroxyphenyl)-5-oxoheptan-3-yl]oxy]oxane-3,4,5-tris(olate); tris(ethane), ZINC67903416 - (2R,3R,4S,5S,6R)-2-[(1S,2R)-3-hydroxy-1-(3-hydroxy-4-methoxy-phenyl)-[4-[(E)-3-hydroxyprop-1-enyl], ZINC67911943 - (4S,5Z,6S)-5-[2-[(E)-3-(4-hydroxy-3-methoxy-phenyl)prop-2-enyl]oxyethylidene]-4-(2-methoxy-2-oxo-ethyl), ZINC70665802 - (2S,3S,4R,5R,6R)-5-amino-2-(aminomethyl)-6-(((2R,3S,4R,5S)-5-(((1R,2R,3S,5R,6S)-3,5-diamino-2-(((2R,3R,4R,5S,6R)-3-amino-6-(aminomethyl)-4,5-dihydroxyl tetrahydro-2H-pyran-2-yl)oxy)-6-hydroxycyclohexyl); oxy)-4-hydroxy-2-(hydroxymethyl)tetrahydrofuran-3-yl). The 2D representation of the selected best hits is shown in fig. 1.

In order to validate our docking results, we performed another protein-protein docking with the LRP6 and MESD (Mesoderm development) chaperone. MESD is a specialized molecular chaperone for members of the low-density lipoprotein receptor (LDLR) family^[30]. MESD is known as a universal inhibitor for LRP5 and LRP6 proteins^[31]. Thus, we docked the MESD (pdb id - 2KGL) domain in the active site of the LRP6 protein and we analyzed the important interactions. Interestingly, we found salt bridges in Arg792 and Glu708 which are commonly observed in LRP6-ligands interactions. From this analysis, we concluded that the identified lead compounds can efficiently inhibit the LRP6 and DKK1 proteins. The best LRP6-MESD interaction orientation is displayed in fig. 2.

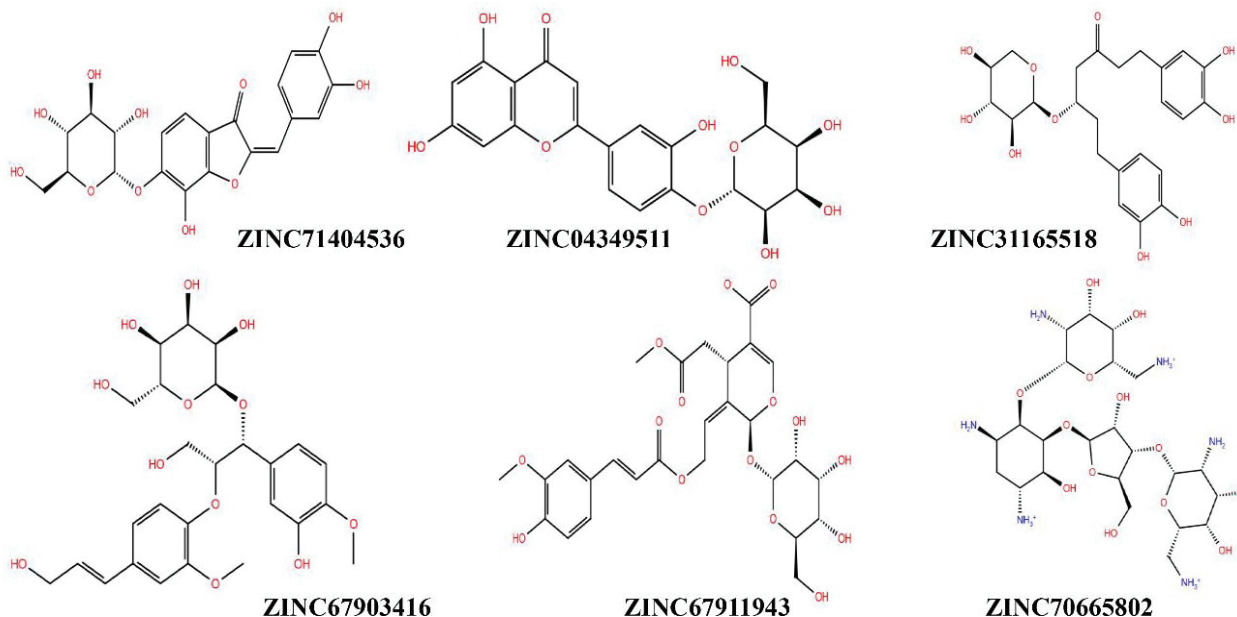


Fig. 1: The 2D representation of all the screened lead molecules.

Additionally, we performed a similarity search for the six identified lead molecules against the drug bank database compounds. The drug bank database contains detailed drug data with comprehensive drug targets. We could not find any similarity of the ligands with the drug bank molecules. Thus we concluded that the identified lead molecules may not bind with other protein targets.

The comparative docking analysis of the six lead compounds including (i) zinc_70665802 (ii) zinc_67903416 (iii) zinc_67911943 (iv) zinc_04349511 (v) zinc_71404536, and (vi) zinc_31165518 against the two molecular target proteins (LRP6 and DKK1) of AD were performed using the Glide XP application. The glide scores for zinc database ligands interacted with LRP6 varied from -8.23 kcal/mol to -7.027 kcal/mol, while in the case of DKK1 it ranged from -9.68 kcal/mol to -7.98 kcal/mol. By comparing their respective Glide scores, Glide energies, and hydrogen bond interactions, it was found that all the six compounds exhibited better binding energies in both the targets.

In the LRP6 models compound_71404536 has four interactions. The oxygen atom of the carboxyl group (C=O) from Glu708 interacts with the hydrogen atom of the hydroxyl group (-OH) of compound (C=O...OH, 2.07 Å). The oxygen atom of the hydroxyl group (-OH) from Ser665 interacts with the hydrogen atom of the hydroxyl group (-OH) of compound (OH...OH, 1.73 Å). The hydrogen atom of the (NH) group from Arg751 is well interacted with the oxygen atom of the hydroxyl group (-OH) (NH...OH, 2.05 Å). The oxygen atom of the carboxyl group (C=O) from the ASN813 is interacted with the hydrogen atom of the

hydroxyl group (-OH) (C=O...OH, 1.96 Å). A π ... π stack pairing^[32] is also observed in the His834 residue of the protein LRP6 (3.46 Å).

In the DKK1 models, there are four interactions. The oxygen atom of the carboxyl group (C=O) from the backbone of Cys220 is well interacted with the hydrogen atom of the hydroxyl group (-OH) of compound (C=O...OH, 2.05 Å). The same interaction occurs with the backbone of Lys222 (C=O...OH, 2.24) and Glu232 (C=O...OH, 2.41 Å). Hydrogen bonds are formed from Arg236 where the H atom of the NH group is interacted with the oxygen atom of the OH from compound_71404536 (NH...OH, 2.08 Å).

In the context of LRP6 models, the oxygen atom of the carboxyl group (C=O) from three different amino acids namely Ala664, Glu708 and Leu810 are well interacted with the hydrogen atom of the hydroxyl group (-OH) of compound_31165518 (C=O...OH; 1.92 Å, 1.952 Å and 1.92 Å). There are two π ... π stack pairings observed in the residues Arg792 and His834 of the protein LRP6.

In the DKK1 models, the oxygen atom of the carboxyl group (C=O) from the backbone of four different amino acids Cys220, Lys222, Glu232, and Leu231 are well interacted with the hydrogen atom of the hydroxyl group (-OH) of compound_31165518 (C=O...OH; 2.05 Å, 2.14 Å, 1.87 Å and 2.13 Å). The hydrogen atom of the (NH) group from three different amino acids Arg224, Ile233, His261 are well interacted with the hydrogen atom of the hydroxyl group (-OH) of compound_31165518 (NH...OH; 1.88 Å, 1.82 Å, and 2.06 Å).

In the LRP6 models, a salt bridge is associated

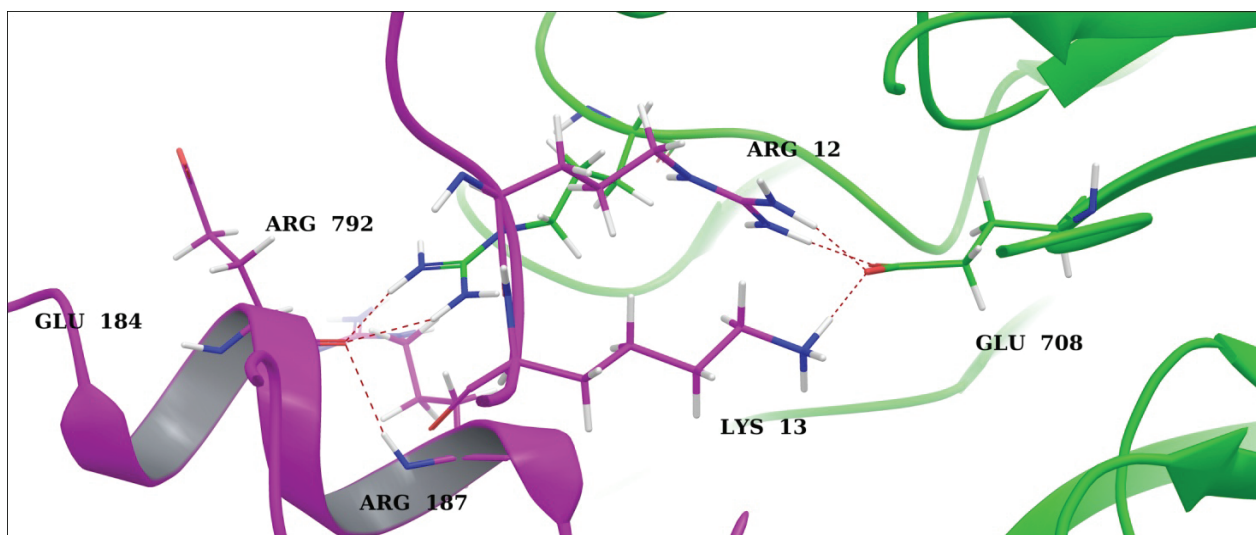


Fig. 2: The best LRP6 – MESD interactions.
(Green color – LRP6; Pink color – MESD)

with Arg792 (4.66 Å). The hydrogen atom of the NH group from Arg792 is interacted with the oxygen atom of the carboxyl group (C=O) of compound_67911943 (C=O...NH; 1.64 Å). Oxygen atom of carboxyl group (C=O) from two different amino acids Glu708 and Arg638 are well interacted with the hydrogen atom of hydroxyl group (-OH) of compound_67911943 (C=O...OH, 1.878 Å and 1.81 Å). A salt bridge is also involved in the amino acid residue Arg792.

In the DKK1 models, a hydrogen atom of the NH group from the backbone of Arg224 is well interacted with the oxygen atom of the carboxyl group (C=O) of compound_67911943 (C=O...NH; 1.84 Å). The oxygen atom of the carboxyl group (C=O) from two different amino acids Lys222 and Cys220 are well interacted with the hydrogen atom of the hydroxyl group (-OH) of compound_67911943 (C=O...OH; 2.05 Å and 2.09 Å). The oxygen atom of the (N=O) group from His261 is interacted with the hydrogen atom of hydroxyl group (-OH) of compound (N=O...OH; 2.04 Å). A π ... π stack pairing is also observed in Phe234.

In the LRP6 models, an oxygen atom of the carboxyl group (C=O) from two different amino acids Pro835 and Glu708 are interacted with a hydrogen atom of the hydroxyl group (OH) of compound_04349511 (C=O...OH; 1.94 Å and 1.87 Å). A hydrogen atom of the NH group from Arg792 is interacted with an oxygen atom of the carboxyl group (C=O) of compound_04349511 (C=O...NH; 2.10 Å). There are two π ... π stacking associated with His834 and Arg792.

In the context of DKK1 models, the oxygen atom of the carboxyl group (C=O) from Leu231 and Glu232 are interacted with the hydrogen atom of

the hydroxyl group (-OH) of compound_04349511 (C=O...OH; 1.953 Å and 1.78 Å). The oxygen atom of the hydroxyl group (-OH) from His261 is interacted with the hydrogen atom of the NH group of compound_04349511 (NH...OH; 2.14 Å).

In the LRP6 models, the oxygen atom of the carboxyl group (C=O) from three different amino acids Glu708, Ser665, and Glu663 are interacted with the hydrogen atom of the hydroxyl group (-OH) of compound_67903416 (C=O...OH; 1.78 Å, 1.96 and 2.02 Å). The hydrogen atom of the NH group from two different amino acids Arg751 and Arg792 are interacted with the oxygen atom of the hydroxyl group (-OH) of compound_67903416 (NH...OH; 1.88 Å and 1.94 Å). π ... π stacking observed in Trp850.

In the DKK1 models, the hydrogen atom of the NH group from four different amino acids Arg236, His261, Arg224, and Lys211 are well interacted with the oxygen atom of the hydroxyl group (-OH) of compound_67903416 (NH...OH; 2.18 Å, 1.81 Å, 2.12 Å and 1.79 Å). The oxygen atom of the carboxyl group (C=O) from two different amino acids Cys220 and Lys222 are interacted with the hydrogen atom of the hydroxyl group (-OH) of compound_67903416 (C=O...OH; 1.96 Å and 1.85 Å). π ... π stacking and π ...cation interaction are observed in the association of Arg236.

In the LRP6 models, the hydrogen atom of the NH group from Arg792 and Glu663 are interacted with the oxygen atom of the carboxyl group (C=O) of compound_70665802 (C=O...NH; 1.83 Å and 1.88 Å). The nitrogen atom of the CN group is interacted with the hydrogen atom of hydroxyl group (-OH) of compound_70665802 (CN...OH; 2.27 Å). π ...cation interaction and salt bridges are observed in Tyr706 and Asp811 respectively.

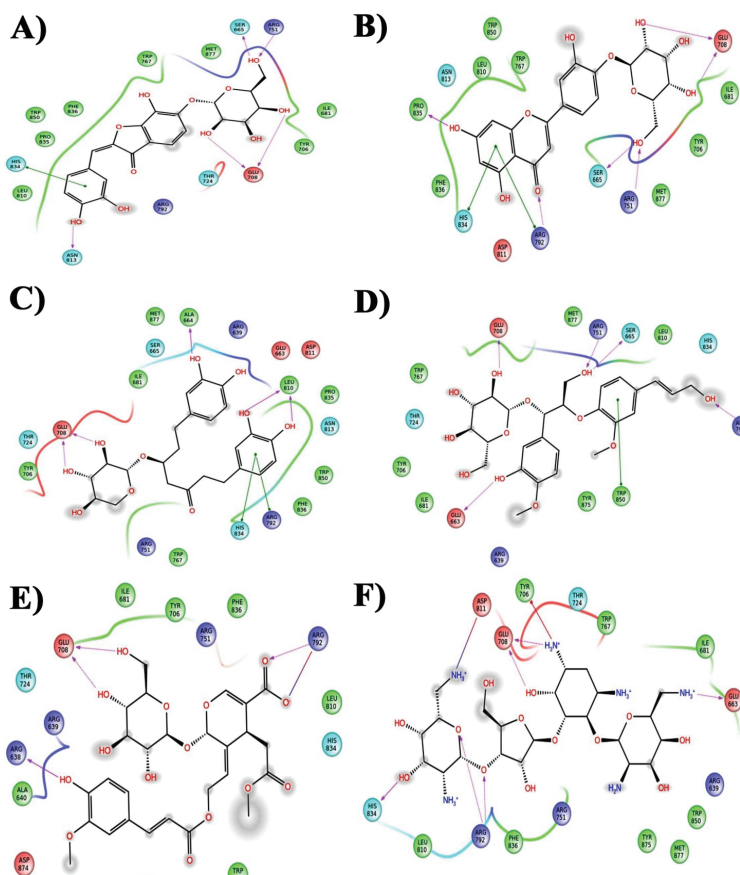


Fig. 4: The 2D interaction diagram for all docked complex in DKK1 active site. (A) ZINC71404536, (B) ZINC31165518, (C) ZINC67911943, (D) ZINC04349511, (E) ZINC67903416, (F) ZINC70665802

TABLE 1: THE COMPARATIVE DOCKING ANALYSIS OF SIX BEST LEAD COMPOUNDS

Ligand	Docking score (kcal/mol)	Glide energy (kcal/mol)	Glide emodel (kcal/mol)	H-bond interaction (D...H...A)	Bond length (Å)
LRP6 MODELS					
ZINC71404536	-8.226	-40.443	-54.518	O-H...C=O (GLU 708) O-H...C=O (GLU 708) OH.....OH (SER 665) N-H...=O-H (ARG751) O-H...C=O (ASN 813) π π (HIS 834)	2.07 1.90 1.73 2.05 1.96 3.46
ZINC31165518	-7.996	-40.869	-54.430	O-H...C=O (LEU 810) O-H...C=O (LEU 810) O-H...C=O (GLU 708) O-H...C=O (GLU 708) O-H...C=O (ALA 664) π π (ARG 792) π π (HIS 834)	1.91 2.34 1.66 1.95 1.92 5.47 3.78
ZINC67911943	-7.288	-41.536	-52.647	N-H...=O-C (ARG 792) O-H...C=O (GLU 708) O-H...C=O (GLU 708) O-H...C=O (ARG 638) Salt Bridge (ARG 792)	1.64 1.78 1.88 1.81 4.66
ZINC04349511	-7.250	-44.365	-59.569	N-H...=O-C (ARG 792) N-H...=O-H (ARG 751) OH.....OH (SER 665) O-H...C=O (PRO 835) O-H...C=O (GLU 708) O-H...C=O (GLU 708) π π (HIS 834) π π (ARG 792)	2.10 2.03 1.72 1.94 2.09 1.86 3.65 5.22
ZINC67903416	-7.083	-49.610	-64.398f	N-H...=O-H (ARG 792) N-H...=O-H (ARG 751) O-H...C=O (GLU 708) O-H...C=O (SER 665) O-H...C=O (GLU663) π π (TRP 850)	1.88 1.94 1.78 1.96 2.02 5.25

ZINC70665802	-7.027	-49.413	-56.714	CN...HO (HIS 834)	2.27
				N-H...=O-C (ARG 792)	1.83
				N-H...=O-C (ARG 792)	2.05
				N-H...=O-C (GLU 663)	1.89
				O-H...C=O (GLU 708)	5.23
				O-H...C=O (GLU 708)	1.80
				π ...Cation (TYR 706)	5.23
				Salt Bridge (ASP 811)	4.27
DKK1 MODELS					
ZINC31165518	-9.678	-46.195	-62.297	N-H...=O-H (ARG 224)	1.88
				N-H...=O-H (ILE 233)	1.82
				N-H...=O-H (HIS 261)	2.06
				O-H...C=O (CYS 220)	2.05
				O-H...C=O (LYS 222)	2.14
				O-H...C=O (LYS 222)	1.89
				O-H...C=O (GLU 232)	1.87
				O-H...C=O (LEU 231)	2.13
				O-H...C=O (CYS 220)	1.96
				O-H...C=O (LYS 222)	1.85
				O-H...C=O (LYS 222)	2.03
				N-H...=O-H (ARG 236)	2.26
				N-H...=O-H (ARG 236)	2.18
				N-H...=O-H (HIS 261)	1.81
N-H...=O-H (ARG 224)	2.11				
N-H...=O-H (LYS 211)	1.79				
π ...Cation (ARG 236)	3.58				
π ... π (ARG 236)	3.55				
ZINC04349511	-8.211	-46.856	-56.123	N-H...=O-C (ARG 224)	1.89
				N-H...=O-H (HIS 261)	2.14
				O-H...C=O (LEU 231)	1.95
				O-H...C=O (GLU 232)	1.78
ZINC71404536	-8.051	-40.562	-56.765	O-H...C=O (GLU 232)	2.03
				O-H...C=O (CYS 220)	2.05
				O-H...C=O (LYS 222)	2.24
				O-H...C=O (GLU 232)	2.41
				N-H...=O-H (ARG 236)	1.96
				N-H...=O-H (ARG 236)	2.26
				N-H...=O-H (ARG 236)	2.08
ZINC70665802	-7.995	-57.033	-77.808	N-H...=O-H (HIS 261)	2.05
				N-H...=O-C (ARG 259)	2.29
				N-H...=O-C (ARG 236)	2.50
				C=O...N=O (ARG 259)	2.02
				N=C...N-H (HIS 261)	2.36
				O-H...C=O (ARG 259)	1.91
				O-H...C=O (CYS 220)	2.10
				O-H...C=O (GLU 232)	1.71
				O-H...C=O (PHE 234)	1.77
				O-H...C=O (LYS 222)	1.83
				π ... π (ARG 224)	5.89
				N-H...=O-H (ARG 236)	2.25
				N-H...=O-H (ARG 236)	2.07
				N-H...=O-C (ARG 224)	1.84
N=O...H-O (HIS 261)	2.05				
ZINC67911943	-7.973	-49.462	-61.776	O-H...C=O (LYS 222)	2.05
				O-H...C=O (CYS 220)	2.09
				π ... π (PHE 234)	3.98

we confirmed that after docking all the selected hits stabilized the protein structure (figs. 5a and 5c).

Ligand flexibility is also assessed by RMSD (root mean square deviation) and Rg (radius of gyration). Three ligands (B) 70665802 (black), (D) 67911943 (red), and (G) 31165518 (navy blue) drifted from 0.1 Å to 0.4 Å in the LRP6 target site. However, two ligands (C) 67903416 (red) and (E) 04349511 (pink) did not show any driftiness from its mean position and stabilized throughout the 5 ns simulation job in the range of 0.1 Å in the protein target site of LRP6.

In the case of DKK1, three ligands, namely (B) 70665802 (black), (D) 67911943 (blue), and (G)

31165518 (navy blue) drifted from its mean position from the range of 0.2 Å to 0.4 Å. However, the ligands (F) 71404536 (green), (C) 67903416 (red) stabilized in the range of 1.5 Å while ligand (E) 04349511 (pink) initially drifted slightly but later stabilized in the range of 1.5 Å.

Instability of the moment of inertia widened in the case of the LRP6 protein target site where ligands (G) 31165518 (navy blue) and (D) 67911943 fluctuated from 0.42 Å to 0.54 Å and from 0.52 Å to 0.54 Å respectively. However, rigidity was also seen in the case of ligand (C) 67903416 (red) and (B) 70665802 (black) in the range of 0.47 Å, while in the case of (E) 04349511 (pink) it stabilized in the range of 0.5 Å.

In the case of DKK1 protein target site, all of ligands fluctuated from the center of mass, showing ligand flexibility. The ligand RMSD of LRP6 and DKK1 is shown in figs. 5b and 5d, respectively.

The radius of gyration (R_g) assesses the stability of the moment of inertia among the group of atoms from their center of mass. On one hand, it gives flexibility to the protein and on the other hand, it gives the accessibility to the ligands toward the target site of protein. Throughout the simulation time of 5ns all the structures are deviated from 2.80 Å to 3.00 Å. Ligand (E) 04349511 (pink) fluctuated widely. Initially it fluctuated upto 2.95 Å. At 3ns, it decreased to 2.80 Å and went beyond the level of 2.95 Å. All the above descriptions, gave sufficient evidence that the LRP6 had flexibility of target site toward its interacting ligands (figs. 6a and 6b).

In the plot of R_g versus time in the case of DKK1, all ligands fluctuated widely throughout the simulation time. A typical nature of ligand (G) 31165518 (navy blue) observed was that all ligands fluctuated between the ranges of 1.24 Å and 1.34 Å while it fluctuated from the range of 1.16 Å to 1.24 Å. This shows the flexible nature of DKK1 (figs. 6c and 6d).

Ligands (E) 04349511, (B) 70665802 & (G) 31165518 showed wide variations of a number of interacting H-bonds from 1 to 7. It showed that these ligands have loose connection with the target protein LRP6 and confer weak intermolecular H-bond interaction (fig. 7a). In the case of DKK1, ligands (D) 67911943 (blue) and (F) 71404536 showed a wide range of H-bond interactions from 9 to 2, while, ligand (G) 31165518

(navy blue) showed H-bond interactions from 0 to 5. It showed weak intermolecular H-bond interaction towards the protein target DKK1 (fig. 7b).

Protein folding is solely dependent on buried hydrophobic amino acids in the protein core. Ligands exposed to the surface area are uniquely dependent on interactions with the solvent and protein core. These parameters are assessed by SASA (Solvent accessible surface area)^[33]. In LRP6, free energy of salvation ranged from 620 to 740 nm² (fig. 8c), while in the DKK1 the salvation free ranged from 150 to 180 nm² (fig. 8d). Both the protein targets LRP6 and DKK1 had good SASA scores.

Some relevant physiochemical and pharmaceutical components that justify the category of drugs are QPlog (P_o/w) (water octanol partition coefficient, QPlogS (aqueous solubility), QPPCaco-2 (apparent Caco-2 cell permeability), QPlogHERG (IC_{50} value for blockage of HERG K⁺ channels), QPPMDCK (MDCK cell permeability in nm/sec), and human oral absorption of a 0 to 100 % scale. All these properties were assessed by the Qikprop module of Schrodinger 9.6. In the human body, estimation of absorption and distribution of drugs are thoroughly assessed by QPlog (P/w) and QPlogS. The predicted values of QPlog (P_o/w) and QPlogS range from -9.260 to -0.152 and from -2.039 to 2.000 respectively. Caco-2 cells are the model for the gut-blood barrier. Several types of nonactive transports were widely assessed by Caco-2 cell permeability. Its values range from 0.006 to 15.451. Drugs can metabolize and access to biological membranes only when the IC_{50} value for

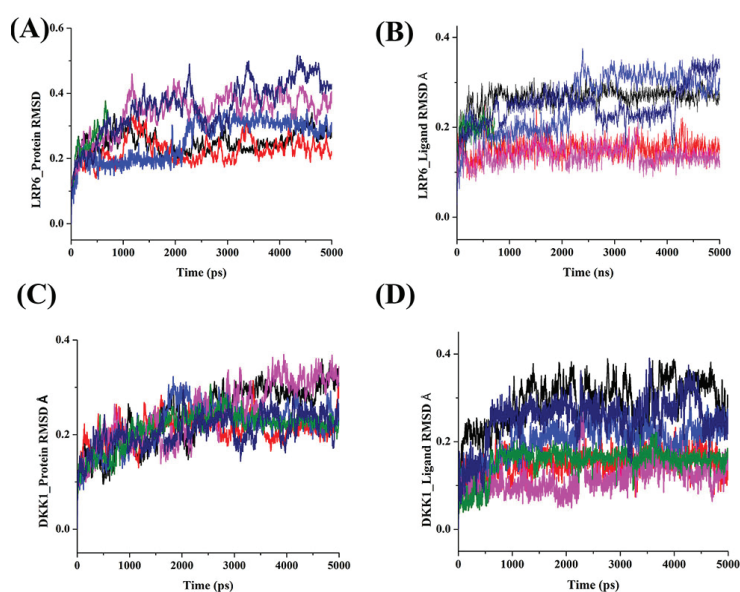


Fig. 5: RMSD versus time plot for ligands. Time evolution of backbone RMSD of LRP6 models (A) and DKK1 models (B) and lead molecules in the active site of LRP6 (C) and DKK1 (D)

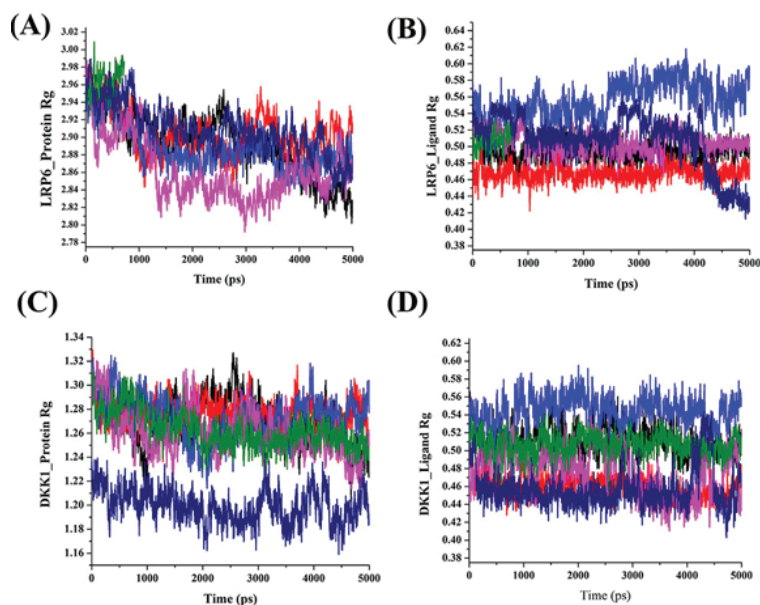


Fig. 6: Time evolution of protein gyration.

Time evolution of protein gyration of LRP6 models (A) and DKK1 models (B) and lead molecules in the active site of LRP6 (C) and DKK1 (D)

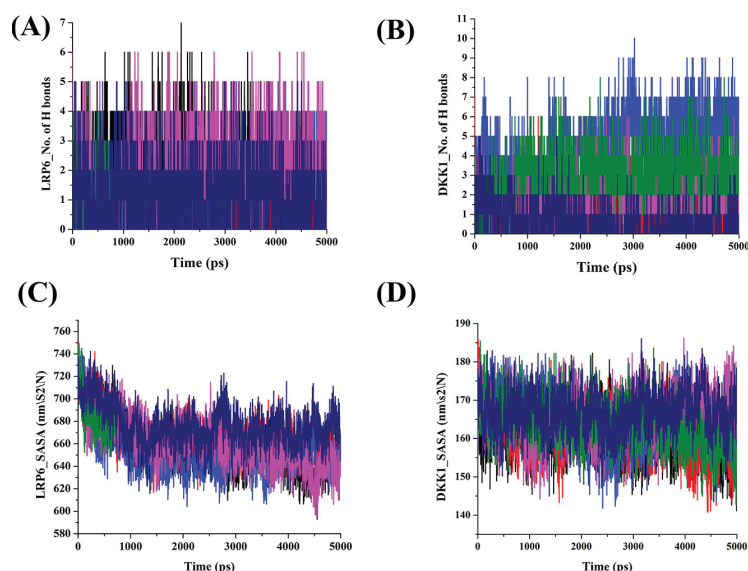


Fig. 7: Total number of hydrogen bonds and solvent accessible surface area for ligands at active site.

Total number of hydrogen bonds in the active site of (A) LRP6 and (B) DKK1 and calculated solvent accessible surface area for LRP6 (C) and DKK1 (D)

TABLE 2: PREDICTED PHYSICOCHEMICAL DESCRIPTORS CALCULATED BY QIKPROP SCHRODINGER 9.6

Lead Molecules ^a	QPlog(P _o /w) ^b	QPlogS ^c	QPCCaco ₂ ^d	QPlogHERG ^e	QPPMDCK ^f	% Human oral absorption ^g
71404536	-1.12	-2.51	8.99	-5.62	3.04	11.54
31165518	-0.15	-3.33	3.68	-6.40	1.16	23.22
67911943	-0.45	-2.88	1.04	-4.13	0.37	0.000
04349511	-0.70	-2.96	7.46	-5.61	2.48	12.51
70665802	-0.29	-2.03	15.45	-5.09	5.46	7.68
67903416	-9.26	2.00	0.006	-8.89	0.002	0.001

^a Ligand IDs are from ZINC database, ^b predicted octanol/water partition coefficient (-2.0-6.5), ^c predicted aqueous solubility, log S. S in moldm⁻³ is the concentration of the solute in a saturated solution that is in equilibrium with the crystalline solid (-6.5-0.5), ^d predicted apparent Caco-2 cell permeability in nm/sec. Caco-2 cells are a model for the gut- blood barrier. QikProp predictions are for non-active transport (<25 poor, >500 great), ^e predicted IC₅₀ value for blockage of HERG K⁺ channels (concern below -5), ^f predicted apparent MDCK cell permeability in nm/sec. MDCK cells are considered to be a good mimic for the bloodbrain barrier. QikProp predictions are for non-active transport (<25 poor, >500 great), ^g predicted human oral absorption on 0 to 100 % scale. The prediction is based on a quantitative multiple linear regression model. This property usually correlates well with human-oral-absorption, as both measures the same property (>80 % is high <25 % is poor).

blockage of HERG K⁺ channels are appropriate. The predicted values of QPlogHERG range from -8.889 to -4.129. The blood-brain barrier accessibility of drugs is assessed by QPPMDCK because it is a good mimic for the blood-brain barrier. The predicted

values of QPPMDCK range from 0.002 to 5.455. Predicted values of percent human oral absorption ranged from 0.000 to 23.219. The predicted ADME property results are shown in Table 2.

Molecular docking and dynamics simulation reports

clearly indicate that the reported six lead molecules inhibit binding of the LRP6 and DKK1 protein complexes. All the reported ligand molecules have good Glide scores, Glide energy, and further they were confirmed with the molecular dynamics simulation studies. Of the six best ligands, the following two ligands satisfied the different molecular docking and druggable properties. The ligand 67911943 had the best Glide score, satisfied the ADME descriptor QPlog HERG, and showed higher deviations in radius of gyration plot for both the proteins (LRP6 and DKK1). It also confirmed the ease of accessibility in the active site of the protein. Another ligand 67903416, also not deviated from its mean position in RMSD of both the LRP6 and DKK1 plots, conferred its least conformational driftness and better binding trends towards the active site of protein. Stack pairing, π -cation pairing, and salt-bridges are important non-covalent interactions which give the overall stabilizations to the protein-ligand complexes. All the six reported ligands interacted with LRP6 and DKK1 proteins through the above said interactions. π - π stack pairings were observed in the residues His834, Arg792, and Trp850 in the LRP6 hydrophobic patch and Arg236 and Arg224 were involved in the DKK1 active site. π - Cation pairing was observed in Tyr706 in LRP6 and Arg236 in DKK1, while salt bridges were observed in Asp 811 and Arg792 in the LRP6. His834, Trp850, and Tyr706 are the hydrophobic patch residues of LRP6 while Arg236 and Arg224 are the active site residues of DKK1. This interprets that ligands have bound nicely to their respective protein target sites. The scores of SASA are better in LRP6 (740nm²) rather than in DKK1 (180nm²). Thus, solvation energy, and exposed surface for binding to ligands are high in LRP6 rather than in DKK1. The radius of gyration is also high in LRP6 rather than in DKK1, which gives further flexibility to the concerned protein and better accessibility to its interacting ligands. Overall analysis of all the parameters show that all the compounds bind better in the LRP6 target site rather than in DKK1, which will be used for the treatment of late onset AD.

FINANCIAL ASSISTANCE

None.

CONFLICT OF INTERESTS

None declared.

REFERENCES

- Hardy J, selkoe DJ The amyloid hypothesis of alzheimer's disease: progress and problems on the road to therapeutics. *Science* 2002;297:353-6.
- SerranoPozo A, Frosch MP, Masliah E, Hyman BT. Neuropathological alterations in Alzheimer disease. *Cold Spring Harb Perspect Med* 2011;1: a006189.
- Hendrie HC, Ogunniyi A, Hall KS, Baiyewu O, Unverzagt FW, Gureje O, *et al.* Incidence of dementia and Alzheimer disease in 2 communities: Yoruba residing in Ibadan, Nigeria, and African Americans residing in Indianapolis, Indiana. *JAMA* 2001;285:739-47.
- Ferri CP, Prince M, Brayne C, Brodaty H, Fratiglioni L, Ganguli M, *et al.* Global prevalence of dementia: A Delphi consensus study. *Lancet* 2005;366:2112-7.
- Evans DA, Hebert LE, Beckett LA, Scherr PA, Albert MS, Chown MJ, *et al.* Education and other measures of socioeconomic status and risk of incident Alzheimer disease in a defined population of older persons. *Arch Neurol* 1997;54:1399-405.
- Ogunniyi A, Baiyewu O, Gureje O, Hall KS, Unverzagt F, Siu SH, *et al.* Epidemiology of dementia in Nigeria: Results from the Indianapolis-Ibadan study. *Eur J Neurol* 2000;7:485-90.
- Lambert JC, Wavrant-DeVri ze F, Amouyel P, Chartier-Harlin MC. Association at LRP gene locus with sporadic late-onset Alzheimer's disease. *Lancet* 1998;351:1787-8.
- Arelin K, Kinoshita A, Whelan CM, Irizarry MC, Rebeck GW, Strickland DK, *et al.* LRP and senile plaques in Alzheimer's disease: colocalization with apolipoprotein E and with activated astrocytes. *Brain Res Mol Brain Res* 2002;104:38-46.
- Moir RD, Tanzi RE. LRP-mediated clearance of A β is inhibited by KPI-containing isoform of APP. *Curr Alzheimer Res* 2005;2:269-73.
- Bu G, Cam J, Zerbinatti C. LRP in amyloid-beta production and metabolism. *Ann NY Acad Sci* 2006;1086:35-53.
- Deane R, Sagare A, Zlokovic B. The Role of the Cell Surface LRP and Soluble LRP in Blood-Brain Barrier A β Clearance in Alzheimer's Disease. *Curr Pharm Des* 2008;14:1601-5.
- Meijer AB, Rohlena J, van der Zwaan C, van Zonneveld AJ, Boertjes RC, Lenting PJ, *et al.* Functional duplication of ligand binding domains within low-density lipoprotein receptor-related protein for interaction with receptor associated protein, alpha2-macroglobulin, factor IXa and factor VIII. *Biochim Biophys Acta* 2007;774:714-22.
- Cheng Z, Biechele T, Wei Z, Morrone S, Moon RT, Wang L, *et al.* Crystal structures of the extracellular domain of LRP6 and its complex with DKK1. *Nat Struct Mol Biol* 2012;18:1204-10.
- Singh KD, Karthikeyan M, Kirubakaran P, Sathya V, Nagamani S. Structure-based drug discovery of APOE4 inhibitors from the plant compounds. *Med Chem Res* 2012;21:825-33.
- Berman HM, Westbrook J, Feng Z, Gilliland G, Bhat TN, Weissing H, *et al.* The Protein Data Bank. *Nucleic Acids Research* 2000;28:235-42.
- Jorgensen WL, Maxwell DS, Rives JT. Development and testing of the OPLSAll-Atom Force Field on Conformational Energetics and Properties of Organic Liquids. *J Am Chem Soc* 1996;118:11225-36.
- LigPrep. 2011. Version 2.5, Schrodinger, LLC, New York.
- Friesner RA, Banks JL, Murphy RB, Halgren TA, Klicic

- JJ, Mainz DT. Glide: A new approach for rapid, accurate docking and scoring. 1. Method and assessment of docking accuracy. *J Med Chem*. 2004;47:1739-49.
19. Nagamani S, Muthusamy K, Kirubakaran P, Singh KD, Krishnasamy G. Theoretical studies on benzimidazole derivatives as *E. coli* biotin carboxylase inhibitors. *Med Chem Res*. 2012;21:2168-80.
 20. Kirubakaran P, Muthusamy K, Singh KD, Nagamani S. Homology modeling, molecular dynamics, and molecular docking studies of *Trichomonas vaginalis* carbamate kinase. *Med Chem Res*. 2012;21:2105-16.
 21. QikProp. 2011. Version 3.4, Schrodinger, LLC, New York.
 22. Lipinski CA, Lombardo F, Dominy BW, Feeney PJ. Experimental and computational approaches to estimate solubility and permeability in drug discovery and development settings *Adv Drug Deliv Rev*. 2001;3:26.
 23. Van Der Spoel D, Lindahl E, Hess B, Groenhof G, Mark AE, Berendsen HJ. GROMACS: fast, flexible, and free. *J Comput Chem* 2005;26:1701-8.
 24. Essman U, Perela L, Berkowitz ML, Darden T, Lee H, Pedersen LG. A smooth particle mesh Ewald method. *J Chem Phys* 1995;103:8577-92.
 25. Berendsen HJC, Postma JPM, Di Nola A, Haak AR. Molecular dynamics with coupling to an external bath. *J Chem Phys* 1984;81:3684-90.
 26. Arrinello M, Rahman A. Polymorphic transition in single crystals: a new molecular dynamics method, *J Appl Phys* 1981; 52:7182-90.
 27. Petrova SS, Solovev AD. The origin of the method of steepest descent. *Historia Mathematica* 1985;24:361-75.
 28. Hess B, Bekker H, Berendsen HJC, Fraaije JGEM. LINCS: A linear constraint solver for molecular simulations. *J Comput Chem* 1997;18:1463-72.
 29. Irwin JJ, Shoichet BK. ZINC- A Free Database of Commercially Available Compounds for Virtual Screening. *J ChemInf Model* 2005;45:171-82.
 30. Li Y, Lu W, He X, Bu G. Modulation of LRP6-mediated Wnt signaling by molecular chaperone Mesd. *FEBS Lett* 2006;580:5423-28.
 31. Lu W, Liu CC, Thottassery JV, Bu G, Li Y. Mesd Is a Universal Inhibitor of Wnt Coreceptors LRP5 and LRP6 and Blocks Wnt/ β -Catenin Signaling in Cancer Cells. *Biochemistry* 2010;49:4635-43.
 32. Claessens CG, Stoddart JF. Review commentary π - π interactions in self-assembly. *J Phys Org Chem* 1997;10:254-72.
 33. Durham E, Dorr B, Woetzel N, Staritzbichler R, Meiler J. Solvent accessible surface area approximations for rapid and accurate protein-protein prediction. *J Mol Model* 2009;15:1093-108.

Accepted 16 Apr 2016
Revised 07 Mar 2016
Received 12 Nov 2014
Indian J Pharm Sci 2016;78(2):240-251